ELSEVIER

Journal of Photochemistry and Photobiology
A: Chemistry 87 (1995) 181–191

Journal of
PHOTOCHEMISTRY
AND
PHOTOBIOLOGY
A:CHEMISTRY

The effect of photoirradiation on high-yield pulps: spectroscopy and kinetics

Henrik Tylli [a,*], Ingegerd Forsskåhl [b], Carola Olkkonen [a]

[a] *Department of Chemistry, University of Helsinki, P.O. Box 19, FIN-00014 Helsinki, Finland*
[b] *The Finnish Pulp and Paper Research Institute, Paper Science Centre, P.O. Box 70, FIN-02151 Espoo, Finland*

Received 7 September 1994; accepted 27 September 1994

Abstract

Fluorescence, UV–visible reflectance and diffuse reflectance IR Fourier transform spectroscopy were used to study the changes caused by photoirradiation of unbleached, peroxide-bleached and ozone-bleached mechanical and chemimechanical pulps. Irradiations were performed selectively at 350 nm and emission spectra were obtained using the same excitation wavelength. Kinetic curves were obtained by plotting the integrated emission intensity against the irradiation time. Different domains of photochemical behaviour were observed for unbleached and ozone-bleached mechanical pulps. For peroxide-bleached samples, an exponential decay of the emission intensity was observed on irradiation, accompanied by a shift in the emission maximum to longer wavelengths. The observed emission spectra were deconvoluted into several components, and attempts were made to identify the chromophores causing the emission by comparison with the fluorescence spectra of model compounds.

Keywords: Photoirradiation; High-yield pulps; Spectroscopy; Kinetics

1. Introduction

High-yield pulps contain mainly cellulose, hemicellulose and lignin, i.e. basically the same constituents as wood. Using modern techniques, it is possible to bleach such pulps to high brightness. The main barrier to the more extensive use of bleached lignin-containing pulps in high-value paper is their tendency to yellow on exposure to light. The detailed mechanism of the light-induced yellowing of lignin-containing pulp and paper is still not properly understood. The present knowledge concerning the mechanisms of photoyellowing has been reviewed recently by Heitner and Schmidt [1]. The predominant role of lignin in the photochemical discolouration process has been convincingly demonstrated [2–6], although the significance of the carbohydrate components in colour formation should be kept in mind [7,8], especially for irradiation wavelengths shorter than 300 nm [9]. High-yield pulps are often bleached with chlorine-free reagents such as oxygen and hydrogen peroxide. Today, chemical pulps are also bleached with ozone and peroxide in new bleaching processes with multistage ozone and peroxide sequences. It is mainly the lignin component which responds to bleaching, although cellulose and hemicellulose are also affected to a certain extent. Our understanding of the actions of the various oxygen-containing, chlorine-free bleaching agents at the molecular level is clearly insufficient. However, there seems to be little doubt that the chemical modification of lignin which occurs during bleaching also influences the light-induced yellowing of both mechanical (lignin-rich) and chemical (containing only residual lignin) pulps.

We have recently reported results from the irradiation of cellulose [9]. In this report, we present a systematic study of the effect of irradiation at 350 nm on pressure groundwood (PGW) and chemimechanical pulp (CMP) and on these pulps bleached with hydrogen peroxide and ozone. An attempt was made to identify some of the compounds that may be responsible for the fluorescence observed from these samples. This was done by performing deconvolutions of the emission bands and by measuring the emission spectra of suitable model compounds.

2. Experimental details

2.1. Sample preparation

PGW samples were made from fresh spruce (*Picea abies*) by pressurized grinding in a 110 kW pilot grinder

---

[*] Corresponding author.

SSDI 1010-6030(94)03971-2

with a stone width of 120 mm and diameter of 500 mm. The pulp was washed with ethylenediaminetetraacetic acid (EDTA) solution (2 g l^{-1}) and thick sheets (approximately 400 g m^{-2}) were prepared in deionized water.

Peroxide-bleached samples of PGW (PGWB) were made by bleaching the corresponding pulp with a solution containing 4% hydrogen peroxide, 3.4% sodium hydroxide and 0.2% diethylenetriaminepentaacetic acid (DTPA), with 0.05% magnesium sulphate and 3.5% sodium silicate as stabilizers. Bleaching was performed at 15% consistency, with a bleaching temperature of 65 °C and a reaction time of 3 h. The bleached pulps were washed with EDTA solution (2 g l^{-1}) and deionized water.

CMP was made as described previously [10], and peroxide-bleached CMP (CMPB) was made by bleaching CMP as described above.

Ozone-bleached samples of PGW (PGWZ) and CMP (CMPZ) were made by treating the corresponding pulp with 1% ozone without adjustment of the pH at a consistency of 12.5%. The reaction time was 25 min, the starting pH was 4.1 and the final pH at the end of the reaction was 6.5. During the treatment the temperature increased from ambient to about 35 °C due to the occurrence of exothermic reactions. The bleached pulps were treated as the PGW pulps above and thick sheets (approximately 400 g m^{-2}) and thin sheets (15–20 g m^{-2}) were prepared. The characteristics of the pulp samples are shown in Table 1.

2.2. *Spectroscopic measurements*

Fluorescence spectra were obtained with a Shimadzu RF-5001PC spectrofluorometer using 350 nm excitation and a bandwidth of 3 nm. Appropriate filters were used on both the excitation and emission sides. The same scattering geometry and the same filters were used throughout the measurements. The emission properties of various samples were monitored as a function of the irradiation time over extended time periods. The sample position was not changed during the measurements. The emission spectra shown in this study were not corrected for the wavelength dependence of the emission monochromator efficiency or the detector response. However, this introduces only a small and constant distortion of the emission band shape because the same excitation wavelength (350 nm) was used and the same wavelength range (350–650 nm) was studied in all cases. Further experimental details are given elsewhere [10].

Table 1
Characteristics of unirradiated and irradiated pulp samples

Pulp	Brightness (%)			Heavy metals (ppm)		
	0 h	5 h	20 h	Fe	Mn	Cu
PGW	70.2	64.3	54.0	6.21	0.68	0.33
PGWB	82.6	68.2	56.5	8.94	0.47	0.06
PGWZ	66.8	59.5	49.8	20.8	0.29	0.40
CMP	74.3	54.2	49.2	27.6	2.29	14.7
CMPB	81.9	56.2	50.6	29.5	0.77	5.64
CMPZ	68.7	57.5	48.7	31.6	0.29	4.28

Kinetic curves were constructed by plotting the apparent emission intensity obtained as the area under the curve against the irradiation time.

UV–visible reflectance spectra were measured in the wavelength range 250–750 nm with a Perkin–Elmer Lambda 15 instrument equipped with an integrating sphere. Difference spectra were calculated by subtracting the spectrum of the treated pulp from the spectrum of the untreated pulp.

Fourier transform diffuse reflectance (DRIFT) spectra were measured with a Nicolet 740 instrument using a circular sampling area with a diameter of 1 mm.

2.3. *Curve fitting*

In order to perform meaningful deconvolution of the observed emission bands into components, the shape of the individual components must be known. Due to the mirror symmetry which is frequently observed between the absorption and fluorescence spectra, the band shape should be the same in both cases if instrument-related factors are compensated for. Inspection of the spectra of complex molecules reveals that the bands always show a certain amount of skewness [11,12]. Although the main features of an absorption or emission band of a complex molecule may be described by a gaussian function, increasing systematic deviation from the gaussian band shape is observed in the wings of the band [13,14]. This is true even in the absence of instrument distortion. The deviation is probably due to the anharmonicity of the molecular vibrations [15] which, through the corresponding Franck–Condon factors, influence the band shape. If the skewness is neglected, there is a danger that a single asymmetric band will be erroneously analysed in terms of several purely gaussian components. The asymmetry of spectral bands can be taken into account by using either the log-normal distribution [16,17] or an exponentially modified gaussian band shape, frequently used in chromatographic applications [18]. The band analysis in this study was performed with PeakFit™ software [19] using exponentially modified gaussian components. The "natural line shape" of the emission obtained with our experimental apparatus was checked by measuring the solution state spectra of several complicated molecules known to exhibit only a single emission band. In each case, curve fitting with a single exponentially modified gaussian band was performed and the band parameters obtained in this way were used in the deconvolution procedure.

3. Results and discussion

3.1. Fluorescence and DRIFT spectroscopy

Samples of PGW display three clearly different domains of behaviour on irradiation at 350 nm. During the first hour of irradiation, a decrease is observed in the emission intensity without any shift in the position of the emission maximum (Fig. 1). The emission band can be deconvoluted into three exponentially modified gaussian components with maxima at 447, 484 and 522 nm (Fig. 2 and Table 2). A small decrease in the intensity of the 447 nm band accounts for the observed intensity decrease in this region. In the second region, extending between 1 and 22 h of irradiation, a broadening of the emission band, a gradual increase in the emission intensity and a shift in the emission maximum to longer wavelengths occur (see Fig. 1, inset). This observation can be understood in terms of a small and simultaneous intensity increase for the bands centred at 484 and 522 nm. In the third region, for irradiation times longer than 22 h, shown in Fig. 3, a continuous decrease is observed in the amount of chromophores emitting at the shortest wavelength (447 nm), together with a build-up of chromophores emitting with maxima at wavelengths longer than 500 nm. An isosbestic point occurs near 510 nm. Its existence confirms that, in this region, only two chromophores, or perhaps more realistically, two families of closely related chromophores are involved in the process. The deconvolution result for the emission spectrum recorded after an irradiation time of 175 h is shown in Table 2.

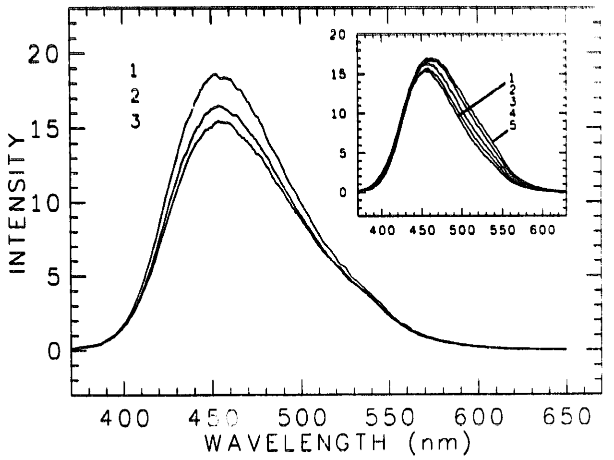

Fig. 1. Luminescence spectra of PGW irradiated at 350 nm in the sample compartment of the spectrometer. Excitation wavelength, 350 nm. The figure shows the first photochemical region. Irradiation times: curve 1, 0 min; curve 2, 15 min; curve 3, 60 min. The inset shows the second photochemical region. Irradiation times: curve 1, 1 h; curve 2, 3 h; curve 3, 6 h; curve 4, 13 h; curve 5, 22 h.

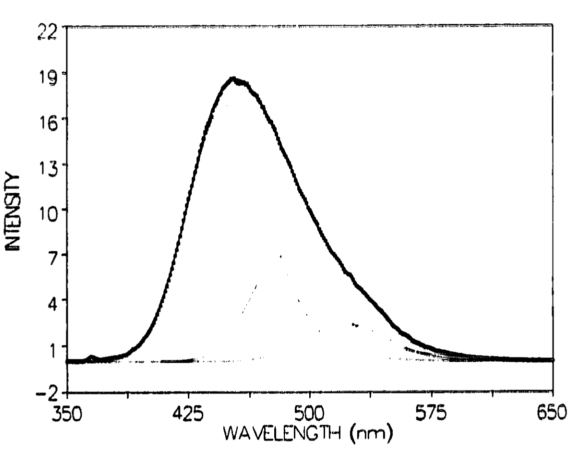

Fig. 2. Luminescence spectrum of unirradiated PGW deconvoluted with three exponentially modified gaussian components.

Pulp samples of PGW treated with ozone (PGWZ) behave in the same way as PGW on irradiation at 350 nm, although the build-up of chromophores emitting around 520 nm is clearer and the isosbestic point (now at 495 nm) is more pronounced for the ozone-bleached sample (see Fig. 3, inset). The deconvolution results are given in Table 2. The ozone treatment obviously affects the chromophore distribution; the decrease in the proportion of the component emitting at short wavelengths leads to a more pronounced appearance of the isosbestic point. Additional experiments were performed with GW sheets treated with ozone for 4 and 24 h. The ozone treatment causes an increase in the width of the emission band, a shift of the band maximum to longer wavelengths and a small increase in the emission intensity.

Samples of PGW bleached with hydrogen peroxide (PGWB) display slightly different emission spectra and behave differently on irradiation at 350 nm. The peroxide-bleached samples show a higher apparent emission intensity, the emission maximum is at a shorter wavelength and a clear shoulder is seen on the short-wavelength side of the emission band (Fig. 4). The spectrum can be deconvoluted into four exponentially modified gaussian components with maxima at 397, 440, 480 and 527 nm (Table 2). Irradiation at 350 nm causes a rapid decrease in the emission intensity and, for longer irradiation times, a shift in the emission maximum to longer wavelengths. The observed shift is caused by a fairly selective consumption of the two short-wavelength components during irradiation. After 50 h of irradiation, a clear isosbestic point develops at around 475 nm.

The emission intensity of CMP is considerably higher than that of PGW and the emission maximum is at a shorter wavelength (10 nm shorter, 443 nm, Fig. 5). This can be understood in terms of a less extensive conjugation for the chromophores in bisulphite-treated pulps. It has been shown by Gellerstedt [20] in a study

Table 2
Results of the peak analysis of the emission spectra

Pulp	Emission maximum	Components							
		λ_{max}	Area (%)	λ_{max}	Area (%)	λ_{max}	Area (%)	λ_{max}	Area (%)
Unirradiated pulps									
PGW	453			447	63.7	484	27.3	522	9.0
PGWZ	459			449	64.0	487	27.3	525	8.6
PGWB	447	397	5.3	440	63.5	480	22.8	527	8.4
CMP	443	397	7.2	435	50.0	469	31.9	519	10.8
CMPZ	447	397	5.2	438	51.9	478	35.2	527	7.6
CMPB	444	396	6.3	435	58.2	472	27.2	521	8.3
Irradiated pulps									
PGW	477	441	19.9	482	57.2	530	22.9		
PGWZ	488	441	17.1	483	61.9	533	21.0		
PGWB	494	446	19.5	493	60.1	536	20.4		
CMP	480	437	19.1	474	42.8	521	38.1		
CMPZ	481	440	19.8	483	64.7	532	15.5		
CMPB	494	434	12.4	479	52.3	529	35.3		

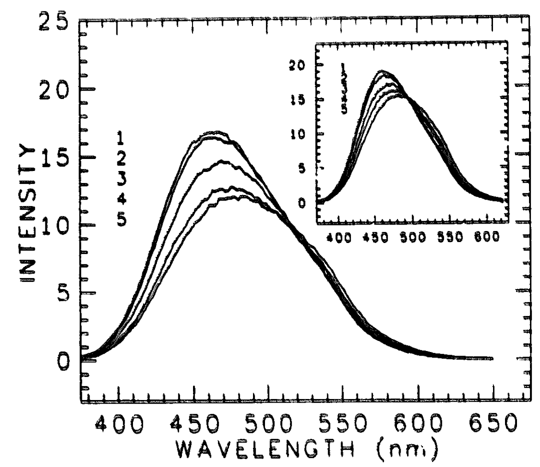

Fig. 3. Luminescence spectra of PGW and PGWZ irradiated at 350 nm showing the third photochemical region. Excitation wavelength, 350 nm. The figure shows the spectra for PGW. Irradiation times: curve 1, 22 h; curve 2, 28 h; curve 3, 55 h; curve 4, 100 h; curve 5, 175 h. The inset shows the spectra for PGWZ. Irradiation times: curve 1, 22 h; curve 2, 28 h; curve 3, 59 h; curve 4, 100 h; curve 5, 175 h.

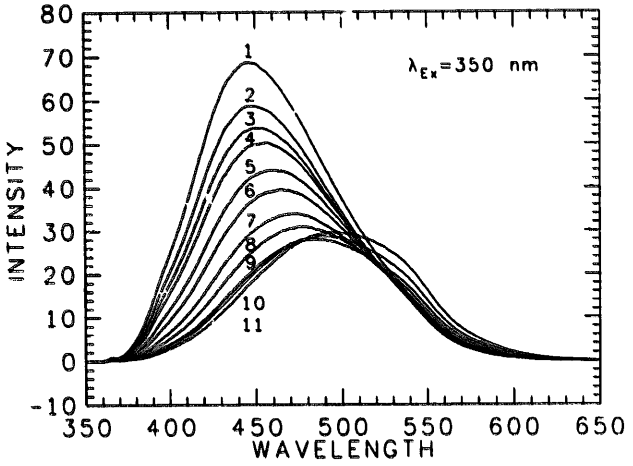

Fig. 4. Luminescence spectra of PGWB irradiated at 350 nm for different times: curve 1, 0 min; curve 2, 10 min; curve 3, 30 min; curve 4, 1 h; curve 5, 3 h; curve 6, 6 h; curve 7, 14 h; curve 8, 26 h; curve 9, 50 h; curve 10, 75 h; curve 11, 150 h.

of model compounds and by Heitner and Min [21] in a study of various chemithermomechanical pulp (CTMP) samples that sulphonation causes destruction of ring-conjugated double bonds. The band shape of the emission also differs markedly from those of PGW and PGWZ, but is similar to that found for PGWB. As for peroxide-bleached PGW, the emission band is considerably broader and a component emitting in the short-wavelength region around 400 nm is clearly seen as a shoulder. Deconvolution of the spectrum yields four bands with maxima at 397, 435, 469 and 519 nm (Table 2). Irradiation of CMP selectively at 350 nm causes a rapid decrease in the emission intensity during the first hour of irradiation, mainly due to consumption of the two short-wavelength components. For longer irradiation times, a gradually increasing shift of the emission maximum to longer wavelengths is observed (see Fig. 5). After an irradiation time of 92 h, the chromophores emitting at 435 nm have reacted almost completely to form reaction products emitting at considerably longer wavelengths.

The emission spectra of CMPZ, irradiated for different times, are shown in Fig. 5 (inset). The emission maximum is at 447 nm and the overall behaviour on irradiation at 350 nm is similar to that found for unbleached CMP, although the light sensitivity of the ozone-bleached sample is higher.

CMPB behaves in the same manner as CMP, although the initial intensity is almost twice as high as that of

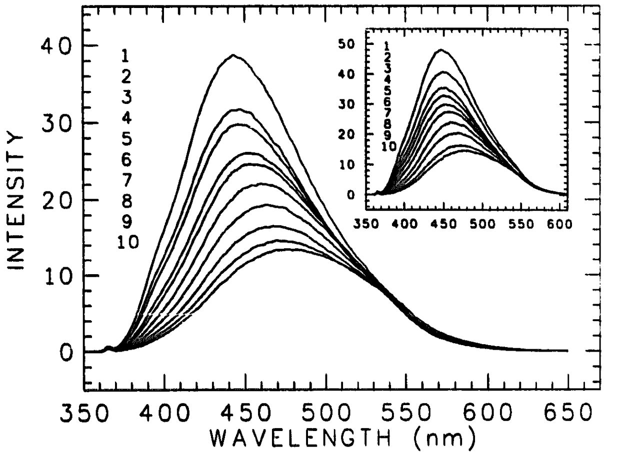

Fig. 5. Luminescence spectra of CMP and CMPZ irradiated for different times at 350 nm. Excitation wavelength, 350 nm. The figure shows the spectra for CMP. Irradiation times: curve 1, 0 min; curve 2, 30 min; curve 3, 1 h; curve 4, 4 h; curve 5, 6 h; curve 6, 12 h; curve 7, 20 h; curve 8, 36 h; curve 9, 58 h; curve 10, 92 h. The inset shows the spectra for CMPZ. Irradiation times: curve 1, 0 min; curve 2, 15 min; curve 3, 30 min; curve 4, 1 h; curve 5, 2 h; curve 6, 5 h; curve 7, 14 h; curve 8, 29 h; curve 9, 67 h; curve 10, 128 h.

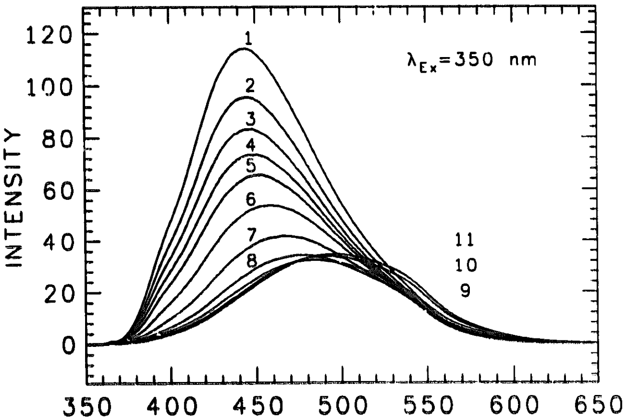

Fig. 6. Luminescence spectra of CMPB irradiated at 350 nm for different times: curve 1, 0 min; curve 2, 5 min; curve 3, 15 min; curve 4, 30 min; curve 5, 1 h; curve 6, 3 h; curve 7, 9 h; curve 8, 24 h; curve 9, 50 h; curve 10, 100 h; curve 11, 145 h.

the unbleached CMP sample (Fig. 6). Deconvolution yields four bands with maxima at 396, 435, 472 and 521 nm. This pulp is extremely light sensitive if irradiated at 350 nm. However, as for PGWB, and contrary to the behaviour of unbleached CMP and CMPZ, an isosbestic point is observed at 470 nm for the peroxide-bleached sample for irradiation times longer than 50 h. After 145 h of irradiation at 350 nm, a strong yellow discolouration is observed in the area exposed to light. DRIFT spectra of the unirradiated and irradiated parts of the sample were recorded. The spectra are shown in Fig. 7 and integrated band intensities and intensity ratios are collected in Tables 3 and 4 respectively. It can be seen that irradiation causes a tenfold intensity increase in the C=O band at 1734 cm^{-1}, a small decrease in the intensity of the C=C double bond absorption at 1645–1547 cm^{-1}, a marked decrease in the intensity of the 1507 cm^{-1} band of the aromatic nucleus and a considerable decrease in the intensity of the 1270 cm^{-1} band. These changes must be attributed to the reactions of hemicellulose and lignin because pure cellulose is not affected if irradiated with light at wavelengths longer than 310 nm [9].

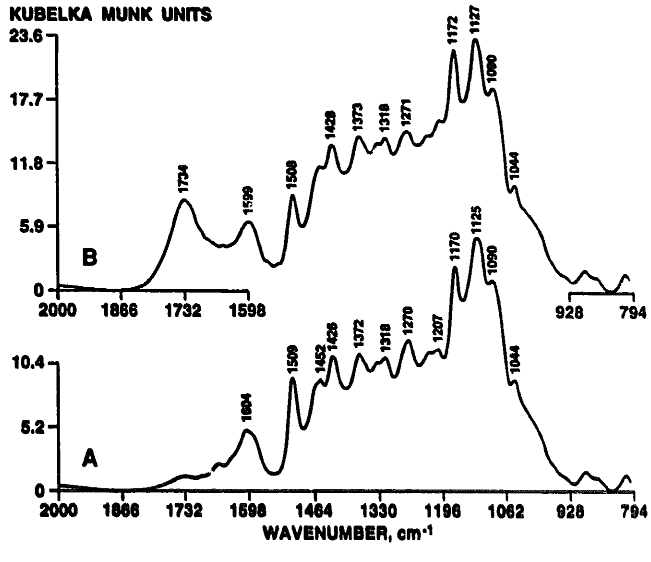

Fig. 7. Diffuse reflectance IR Fourier transform spectra of CMPB samples: spectrum A, unirradiated; spectrum B, irradiated for 145 h at 350 nm.

Table 3
DRIFT absorption band intensities at various frequencies of unirradiated and irradiated peroxide-bleached chemimechanical pulp (CMPB). Irradiation wavelength, 350 nm; irradiation time, 145 h

Frequency range (cm^{-1})	Unirradiated	Irradiated
1192–1151	84.39	98.61
1220–1192	4.65	6.19
1246–1220	3.34	4.18
1300–1246	66.83	45.52
1398–1347	49.62	57.20
1536–1492	99.34	79.02
1645–1547	141.9	133.7
1700–1800	16.25	210.5
3027–2785	810.8	757.7

Kinetic curves, obtained by plotting the apparent total emission intensity (calculated as the area under the emission band) as a function of irradiation time, are shown in Fig. 8. For PGW and PGWZ (curves 1 and 2), the initial small decrease in the intensity during the first hour of irradiation is followed by an exponential increase, observed in the emission spectra as a broadening of the emission band, for irradiation times up to 22 h. For longer irradiation times, a gradual decrease in emission occurs. For PGWB and CMPB (curves 3

Table 4
Ratios between the DRIFT absorption band intensities for certain pairs of frequencies (cm^{-1}) before and after irradiation of peroxide-bleached chemimechanical pulp (CMPB). Irradiation wavelength, 350 nm; irradiation time, 145 h

Pulp	1270/1370	1508/1370	1734/1370	1270/2902	1508/2902	1740/2902
Unirradiated	1.347	2.002	0.327	0.083	0.124	0.020
Irradiated	0.796	1.381	3.680	0.060	0.104	0.278
Change (%)	−40.9	−31.0	+1025	−27.7	−16.1	+1290

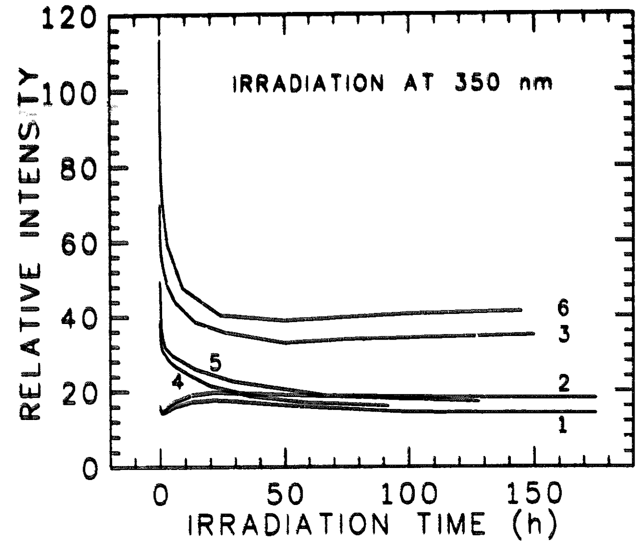

Fig. 8. Change in apparent emission intensity as a function of irradiation time for various pulp samples: curve 1, PGW; curve 2, PGWZ; curve 3, PGWB; curve 4, CMP; curve 5, CMPZ; curve 6, CMPB.

and 6), an initial very rapid decrease in emission is observed during the first few hours of irradiation. The rate of change gradually levels off and, for irradiation times longer than 50 h, a small increase in intensity is observed. The increase in intensity observed for the peroxide-bleached pulps for irradiation times longer than 50 h is evidently due to chromophore precursors formed only as a result of peroxide treatment. CMP and CMPZ (curves 4 and 5) show a similar behaviour on irradiation: an initial rapid decrease in the emission intensity during the first hour of irradiation is followed by a slower decrease on prolonged treatment. For both PGWZ and CMPZ, higher integrated intensities are observed than for the corresponding untreated pulps, and they also level off at slightly higher intensity values on irradiation.

3.2. *UV–visible reflectance spectroscopy*

Treatment of the initial PGW and CMP samples with ozone and peroxide causes different changes in the UV–visible difference reflectance spectra of the pulps. Peroxide treatment is known to bleach groundwood and chemimechanical pulps, as reflected in changes in the spectrum at around 380 and 470 nm [22]. The corresponding changes are seen as minima in curves 3 and 4 in Fig. 9. Ozone (1% solution) causes a weak discolouration; two maxima are observed at 330 and 440 nm for CMP and at 340 and 440 nm for PGW (curves 1 and 2, Fig. 9).

Irradiation of the unbleached and bleached pulps in a Suntest apparatus causes a gradual decrease in the reflectance (R_∞, 457 nm) of the pulps (Table 1, Fig. 10). The rate of discolouration varies, being fastest for the peroxide-bleached CMPs. The light-induced changes are greater for the sulphonated pulps regardless of whether they are bleached or not. The difference between the behaviour of PGWB and CMPB is considerable, particularly after irradiation for 5 h. After long irradiation times (greater than 20 h), the reflectance values approach each other and the effect of bleaching is almost obliterated. The difference between the ozone-treated pulps PGWZ and CMPZ is much smaller, partly because the ozone treatment is considerably milder than the peroxide treatment with regard to the changes in reflectance.

Both the specific absorption coefficient (k), which is directly related to the chromophore content, and the specific scattering coefficient (s) influence the reflectance value (R_∞). To relate the discolouration rates to

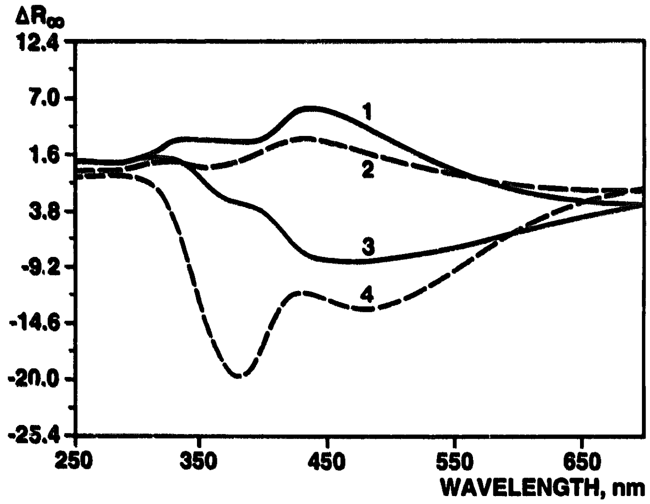

Fig. 9. UV–visible difference reflectance spectra (untreated − treated) of PGW and CMP showing the effect of ozone and peroxide treatment: curve 1, CMPZ; curve 2, PGWZ; curve 3, CMPB; curve 4, PGWB.

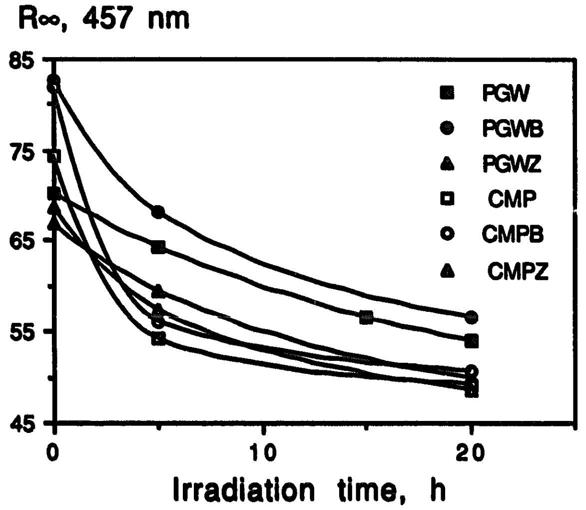

Fig. 10. Reflectance value R_∞ at 457 nm of various pulps as a function of Suntest irradiation time.

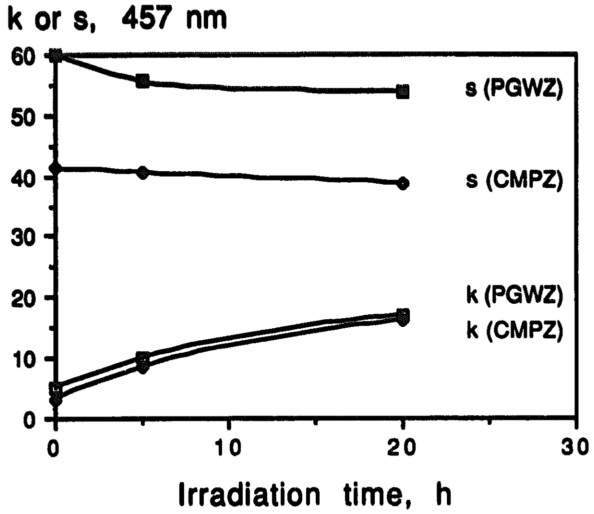

Fig. 11. Values of k and s evaluated at 457 nm of ozone-bleached pulps as a function of Suntest irradiation time.

chromophore changes more clearly, the corresponding k and s values at 457 nm for the ozone-treated pulps PGWZ and CMPZ were evaluated from measurements on thin sheets (Fig. 11). A continuous decrease in scattering at 457 nm is observed during irradiation, but generally the changes are small, particularly for CMPZ. However, for the k values, an increase is observed with irradiation time, and the rate of increase is very similar for the two pulps. The results suggest that sulphonation does not change the rate of formation of chromophores appreciably in ozonized pulps. However, this must be verified using more effective ozone treatment conditions.

Different domains of photochemical behaviour of the pulps are observed using fluorescence spectroscopy. Different behaviour at the beginning and in the later stages of the photoreaction is also observed using UV–visible spectroscopy. During the first 5 h of irradiation, the reflectance at 370 nm of the PGWZ pulp decreases greatly, while the reflectance at 440 nm increases (see Fig. 12, curve 1). On further irradiation, no decrease in reflectance of PGWZ at 370 nm is observed, only a marked broadening of the "yellowing band" at 440 nm (curve 3). Interestingly, the changes for CMPZ are partly similar, although an increase in reflectance at 370 nm is observed for the first 5 h (curve 2), which on longer irradiation is eliminated (curve 4). The 440 nm band is broadened after longer irradiation times, indicating the formation of new reaction products. It is evident that chromophores absorbing around 370 nm are photoreactive at the beginning of the reaction in both PGWZ and CMPZ, and these chromophores are almost totally consumed in the initial phase (0–5 h) of the photoreaction. On prolonged irradiation, the dominant changes in the chromophores occur in those absorbing around 440 nm. At the same time, the rate of change in the chromophore content levels off, which is also seen in the kinetic curves (Figs. 8 and 10).

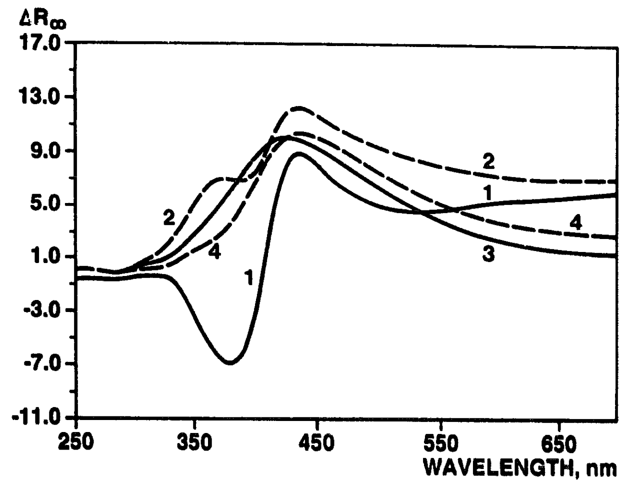

Fig. 12. UV–visible difference reflectance spectra of Suntest-irradiated ozone-bleached pulps: curve 1, PGWZ (irradiated for 5 h) – PGWZ (unirradiated); curve 2, CMPZ (irradiated for 5 h) – CMPZ (unirradiated); curve 3, PGWZ (irradiated for 20 h) – PGWZ (irradiated for 5 h); curve 4, CMPZ (irradiated for 20 h) – CMPZ (irradiated for 5 h).

3.3. Identification of chromophores

It is evident from an inspection of the width and shape of the emission bands, and also from previously published studies, that several chromophores are responsible for the emissions of mechanical and chemimechanical pulps. Even pure cellulose shows a weak background emission [23] which changes with irradiation [9,24]. For high-yield pulps, to this background can be added contributions mainly from the hemicellulose and lignin components and also from the modifications of lignin formed during the pulping and bleaching processes. Castellan et al. [25] obtained different emission spectra from milled wood lignin and peroxide-bleached lignin in solid 2-hydroxypropylcellulose films on excitation at different wavelengths. Zhu and Gray [26] studied the emission spectra of various lignin-containing pulps excited at wavelengths longer than 300 nm and concluded that there was more than one emitting species in the samples.

To account for the observed emission, we need consider only model compounds with extended conjugated systems. We have examined the fluorescence spectra of 26 different model compounds that could serve as candidates for the observed emission. The structures of the compounds studied are shown in Scheme 1 and the results are collected in Table 5 (which should be compared with the deconvolution results shown in Table 2). Of the compounds studied many show an emission spectrum with a maximum at too short a wavelength, indicating that the conjugated system of these compounds is too small. Suitable structures that could account for the short-wavelength component of the emission are the differently substituted cinnamic acids (**5** and **6**), various coumarins (**7**–**9**), flavone-type structures exemplified by compound **10** and the substituted stilbene **23**. For the coumarins **7** and **8**, with a hydroxyl group in the 7-position, a large shift in the emission maximum to longer wavelengths is observed when water is used as solvent instead of ethanol. Doping experiments with 7-hydroxy-4-methylcoumarin (**8**) show, however, that the emission maximum for this compound applied to filter paper is close to the value found in ethanol solution. Cinnamic acid and its analogues play a central role in the formation of various plant phenols. It is also well known that substituted cinnamic acid structures, after hydroxylation in the ortho position with respect to the side chain, followed by an *E*–*Z* isomerization caused by light wavelengths shorter than 360 nm, undergo spontaneous lactonization to form coumarin-type structures [27,28]. Such changes are likely to occur during the production and aging of high-yield pulps. Beyer et al. [29] have previously suggested that 4-hydroxy-3-(1-phenyl)-propylcoumarin, which has an emission maximum at 375 nm, is a model luminophore of the short-wavelength emission of CTMP samples. The second component for which the deconvolution of the emission spectra of the unirradiated pulps yields a λ_{max} value around 440 nm could be accounted for only by one model compound, coniferaldehyde (**4**). This compound shows a rather weak emission with a band maximum at 440 nm.

The two long-wavelength components with deconvoluted band maxima around 480 and 525 nm (Table 2) are not easily accounted for. Oxidative coupling reactions of phenols occur with hydrogen peroxide both in the presence and absence of peroxidases [30–32], yielding coupling products with extended conjugated systems. The coupling of vanillin to dehydrodivanillin (**16**) has been studied [33,34]. Dehydrodivanillin shows a very weak fluorescence with two maxima at 355 and 498 nm. Diferulic acid, which emits in the blue–green region, is formed when synthetic ferulic acid esters of polysaccharides are oxidized with peroxidase–hydrogen peroxide [35]. Bound diferulic acid has also been found in the cell walls of certain plants [36,37].

Phenylcoumaran units, in this work exemplified by dehydrodiisoeugenol (**12**), have been shown to be present in lignin. As shown by an acidolytic method, the number of phenylcoumarans in spruce Björkman lignin has been estimated by Adler and Lundquist [38] to be 25 units for each 100 units of β-O-4. A somewhat higher value, 36 units, based on two-dimensional nuclear magnetic resonance (NMR) measurements, has been reported by Brunow et al. [39]. It has also been shown by Lee and Sumimoto [40] that stilbene-type structures containing hydroxyl groups on both rings, under simulated bleaching conditions with alkaline hydrogen peroxide, yield degradation products and phenylcoumaran in 21% yield. The emission maximum of dehydrodiisoeugenol (**12**) is at 342 nm, which means that unmodified units cannot even account for the short-wavelength component of the observed emission of high-yield pulps. However, different pathways, such as acidolysis [38], may lead from phenylcoumaran to the formation of phenylcoumarone, which has a fairly extensive conjugated system, especially if an unsaturated side chain is present. Castellan et al. [41] have observed that phenylcoumarone units cause a strong discolouration when applied to bleached softwood chemical paper and exposed to UV light. Phenylcoumarans are also known to react with aqueous sodium hydroxide at elevated temperatures to form stilbene-type structures [40]. Therefore, a substituted stilbene (**23**) and a stilbene quinone (**24**) were included among the model compounds studied. Of these, the stilbene (**23**) shows a fairly strong emission at 387 nm, close to the value of 397 nm found for the short-wavelength component of the emission for the unirradiated pulps. The stilbene quinone (**24**) and the lignin-carbohydrate model (**26**) emit at much shorter wavelengths, 310 nm and 313 nm respectively.

The occurrence of pinoresinol-type structures in softwood lignin is well established [42]. The compound (+)-pinoresinol (**25**) emits strongly with a maximum at 310 nm, indicating the two isolated aromatic rings. However, diarylfurofuran lignans react under oxidative conditions to form 4-pyrones [43], with an extended conjugated system, consisting of the two aromatic units linked together via the 4-pyrone ring. Such compounds might well be formed from pinoresinol-type structures and could therefore account for part of the long-wavelength emission.

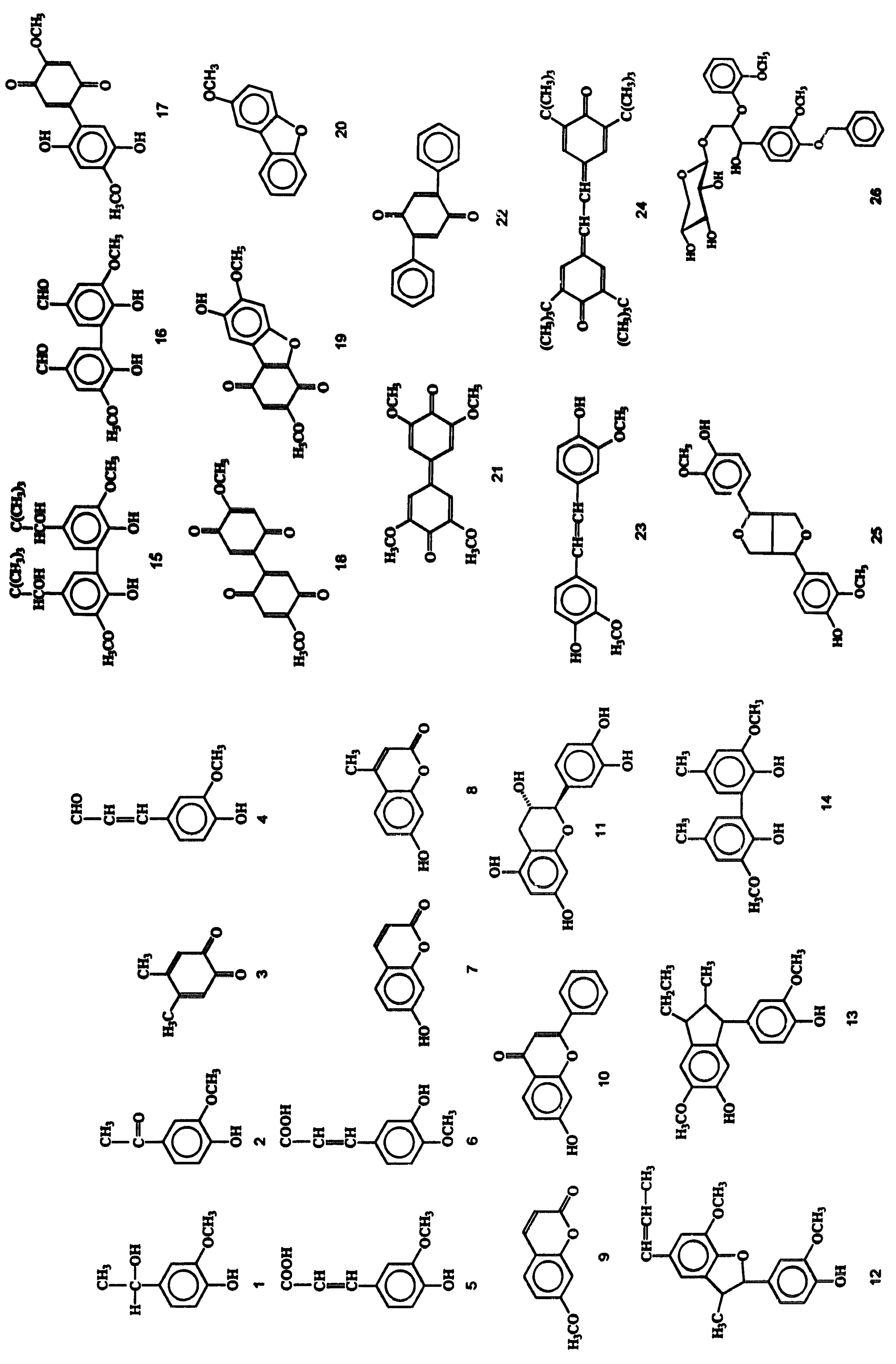

Scheme 1.

Table 5
Emission properties of selected lignin model compounds measured in absolute ethanol solutions. Wavelengths given in parentheses refer to water solutions. Numbering according to Scheme 1

Number	Compound	λ_{Ex} (nm)	λ_{max} (nm)	Intensity
1	Apocynol	270	315	m
2	Acetoguaiacone	330	384	vw
3	4,5-Dimethyl-1,2-quinone	290	322	m
4	Coniferaldehyde	350	440	vw
5	Ferulic acid	350	391	w
6	3-Hydroxy-4-methoxycinnamic acid	330	425	w
7	7-Hydroxycoumarin	320	388 (454)	m
8	7-Hydroxy-4-methylcoumarin	320	384 (449)	m
9	7-Methoxycoumarin	320	384 (390)	m
10	7-Hydroxyflavone	308	400, 521	vw
11	(+)-Catechin	280	316	s
12	Dehydrodiisoeugenol	276	342	w
13	Diisoeugenol	280	324	m
14	Bicreosol	292	379	vs
15	Dehydrodi-tert-butylguaiacylcarbinol	290	376	w
16	Dehydrodivanillin	281	355, 498	vw
17	5-Methoxy-2-(2,5-dihydroxy-4-methoxyphenyl)1,4-quinone	330	434	vw
18	4,4'-Dimethoxybiphenyl-2,5,2',5'-bisquinone	370	440	vw
19	8-Hydroxy-3,7-dimethoxydibenzofuran-1,4-quinone	260	327, 362, 442	vw
20	2-Methoxydibenzofuran	290	345	s
21	Coerulignone	228	345	m
22	2,5-Diphenyl-1,4-benzoquinone	235	379	m
23	3,3'-Dimethoxy-4,4'-dihydroxystilbene	350	387	m
24	3,5,3',5'-Tetra-tert-butylstilbene-4,4'-quinone	240	310	vw
25	(+)-Pinoresinol	277	310	s
26	Lignin-carbohydrate model compound	278	313	vw

m, medium; w, weak; s, strong; v, very.

4. Conclusions

The results obtained from the irradiation of high-yield pulps at 350 nm clearly show the existence of three different photochemical regions for PGW and PGW treated with ozone. In the different regions, the behaviour is determined by different chromophores, which to some extent were pinpointed by the deconvolution of the emission spectra and comparison with the fluorescence spectra of model compounds. Nevertheless, it seems that much basic work still needs to be done before the identification of the various chromophores can be considered complete. This is especially true for those units emitting at longer wavelengths.

Acknowledgements

This project was partly funded by the European Community, Forest Programme, contract no. MA2B-CT-91-0018. We also thank Assoc. Prof. Gösta Brunow for a sample of the lignin-carbohydrate model compound (**26**).

References

[1] C. Heitner and J.A. Schmidt, *Appita, 44* (1991) 131.
[2] P. Nolan, J.A. Van den Akker and W.A. Wink, *Paper Trade J., 121* (1945) 101.
[3] I.H. Spinner, *Tappi, 45* (1962) 495.
[4] S.Y. Lin and K.P. Kringstad, *Tappi, 53* (1970) 658.
[5] U. Tschirner and C.W. Dence, *Pap. Puu, 70* (1988) 338.
[6] U. Tschirner and C.W. Dence, *Pap. Puu, 70* (1988) 345.
[7] D.N.-S. Hon and N. Minemura, in D.N.-S. Hon and N. Shiraisi (eds.), *Wood and Cellulosic Chemistry*, Marcel Dekker, New York, 1991, pp. 395–454, 525–555.
[8] G.C. Ziobro, *J. Wood Chem. Technol., 10* (1990) 151.
[9] H. Tylli, I. Forsskåhl and C. Olkkonen, *J. Photochem. Photobiol. A: Chem., 76* (1993) 143.
[10] H. Tylli, I. Forsskåhl and C. Olkkonen, *J. Photochem. Photobiol. A: Chem., 67* (1992) 117.
[11] H. Voorhof and H. Pollak, *J. Chem. Phys., 47* (1967) 758.
[12] D.B. Siano and D.E. Metzler, *J. Chem. Phys., 51* (1969) 1856.
[13] H. Voorhof and H. Pollak, *J. Chem. Phys., 45* (1966) 3542.
[14] L.P. Kazachenko, *Opt. Spectrosc., 18* (1965) 397.
[15] C.B. Lushchik, N.E. Lushchik and K.K. Shvarts, *Opt. Spectrosc., 9* (1960) 113.
[16] P. Yuan, *Ann. Math. Stat., 4* (1933) 30.
[17] J. Aitcheson, *The Lognormal Distribution*, Cambridge University Press, Cambridge, 1957.
[18] J.A. Jonsson (ed.), *Chromatographic Theory and Basic Principles*, Marcel Dekker, 1987.
[19] PeakFit™ Non-linear Curve-fitting Software, version 3, Program by R. Brown, Jandel Scientific, 1991.

[20] G. Gellerstedt, *Sven. Papperstidn.*, *79* (1976) 537.

[21] C. Heitner and T. Min, *Cellul. Chem. Technol.*, *21* (1987) 289.

[22] I. Forsskåhl and J. Janson, *Nord. Pulp. Pap. Res. J.*, *6* (1991) 118.

[23] S.D. Toner and K.F. Plit, *Tappi*, *45* (1962) 681.

[24] H. Choudhury, S. Collins and R.S. Davidson, *J. Photochem. Photobiol. A: Chem.*, *69* (1992) 109.

[25] A. Castellan, A. Nourmamode, C. Noutary, C. Belin and Ph. Fornier de Violet, *J. Wood Chem. Technol.*, *12* (1992) 19.

[26] J.H. Zhu and D.G. Gray, *J. Photochem. Photobiol. A: Chem.*, *73* (1993) 67.

[27] S.A. Brown, in C.F. Van Sumere and P.J. Lea (eds.), *Ann. Proc. Phytochem. Soc. Europe*, Vol. 25, Oxford University Press, Oxford, 1985, Chapter 14, pp. 257–270.

[28] G.H.N. Towers and E. Yamamoto, in C.F. Van Sumere and P.J. Lea (eds.), *Ann. Proc. Phytochem. Soc. Europe*, Vol. 25, Oxford University Press, Oxford, 1985, Chapter 15, pp. 271–287.

[29] M. Beyer, D. Steger and K. Fischer, *J. Photochem. Photobiol. A: Chem.*, *76* (1993) 217.

[30] K. Freudenberg, *Science*, *148* (1965) 595.

[31] J. Baumgartner and H. Neukom, *Chimia*, *26* (1972) 366.

[32] K.V. Sarkanen and A.F.A. Wallis, *J. Chem. Soc.*, *Perkin Trans. I*, (1973) 1869.

[33] F. Tieman, *Ber.*, *18* (1885) 3493.

[34] E. Bourguelot and L. Marchadier, *C.R. Acad. Sci.*, *138* (1904) 1432.

[35] T. Geissmann and H. Neukom, *Helv. Chim. Acta*, *54* (1971) 1108.

[36] H.U. Markwalder and H. Neukom, *Phytochemistry*, *15* (1976) 836.

[37] R.D. Hartley and E.C. Jones, *Phytochemistry*, *15* (1976) 1157.

[38] E. Adler and K. Lundquist, *Acta Chem. Scand.*, *17* (1963) 13.

[39] G. Brunow, R.M. Ede, K. Lundquist and K. Stern, *Proc. 5th Int. Symp. on Wood and Pulping Chemistry, Raleigh, NC, USA, 1989, TAPPI Proc.*, *2* (1989) 253.

[40] D.Y. Lee and M. Sumimoto, *Holzforschung*, *45* (1991) Suppl. 15.

[41] A. Castellan, N. Colombo, A. Nourmamode, J.H. Zhu, D. Lachenal, R.S. Davidson and L. Dunn, *J. Wood Chem. Technol.*, *10* (1990) 461.

[42] K. Lundquist and R. Strömberg, *Holzforschung*, *42* (1988) 375.

[43] P. Satyanarayana, P. Koteswara Rao, K. Sethuramu, K.N. Viswanatham and S. Venkateswarlu, *Indian J. Chem.*, *30B* (1991) 825.